Nitro-Substituted Bishomocubanes: Synthesis, Characterization, and Application as Energetic Materials

ARTICLE *in* CHEMISTRY - AN ASIAN JOURNAL · DECEMBER 2014

Impact Factor: 4.59 · DOI: 10.1002/asia.201402607 · Source: PubMed

6 AUTHORS, INCLUDING:

Sohan Lal
Indian Institute of Technology Bombay
2 PUBLICATIONS **1** CITATION
SEE PROFILE

Amit Babu Tare
Indian Institute of Technology Bombay
1 PUBLICATION **1** CITATION
SEE PROFILE

Irishi N. N. Namboothiri
Indian Institute of Technology Bombay
139 PUBLICATIONS **1,576** CITATIONS
SEE PROFILE

CHEMISTRY
AN ASIAN JOURNAL
ACES
FULL PAPER

DOI: 10.1002/asia.201402607

Nitro-Substituted Bishomocubanes: Synthesis, Characterization, and Application as Energetic Materials

Sohan Lal,[a] Sundaram Rajkumar,[a, b] Amit Tare,[c] Sasidharakurup Reshmi,[d] Arindrajit Chowdhury,*[c] and Irishi N. N. Namboothiri[a]

Abstract: Several high-energy-density strained polycyclic compounds nitromethyl-l,3-bishomocubane (NMBHC), nitromethylene-1,3-bishomocubane (NMyBHC), and bis(nitromethyl)-1,3-bishomocubane (DNTMBHC), which were synthesized for the first time from bishomocubanone, hold potential for application as standalone fuels in liquid bipropellant systems or as additives in liquid and solid propellant formulations. DFT analysis at the B3LYP/6-31G(d) level of theory was employed to optimize the geometries of the compounds and to determine their densities, heats of formation, and various thermodynamic properties. The density specific impulse, determined by using equilibrium thermodynamics, demonstrated an improvement of 75 s for NMBHC and NMyBHC over standard hydrocarbons. The specific impulse with ammonium perchlorate showed an improvement of 25–30 s over hydroxy-terminated polybutadiene. Thermogravimetric analysis revealed that NMBHC, NMyBHC, and DNTMBHC evaporated readily with activation energies of 58.8, 69.2, and 74.5 kJ mol^{-1}, respectively.

Keywords: cage compounds · energetic materials · fuels · nitro compounds · thermogravimetric analysis

Introduction

High-energy-density materials (HEDMs) are common ingredients in various volume-limited applications that demand high-performance parameters, such as rockets, gas generators, and explosives. An ideal HEDM should possess high gravimetric and volumetric energy densities, a high positive heat of formation (HoF), and a high density, as well as low operational hazards, such as low toxicity, high thermal stability, and low impact sensitivity.[1] Cage hydrocarbons, which form severely strained molecular structures, belong to an interesting class of potential HEDMs. Eaton and Cole[2] synthesized cubane, a polycyclic cage hydrocarbon, which had a density of 1.29 gmcm^{-3}[3] and a high heat of formation (622.1 kJ mol^{-1}),[4] both of which were higher than those of traditional hydrocarbons. Since cubane is a solid, it could either be used in solid propellant formulations as an energetic binder[1] following its conversion into polymeric forms or as an additive in liquid propulsion systems or internal combustion engines. Eaton et al.[5] studied the performance of gasoline that was blended with 30% cubane (v/v) in a single-cylinder engine, thereby demonstrating a 5–6.4% increase in power and a 1.6% decrease in specific fuel consumption.

The strained cage structure of cubane has led researchers to develop similar compounds by modifying its cage structure, as well as by its elaboration with inductive functional groups, such as NO_2, N_3, NF_2, $NHNO_2$, and CH_2NO_2, to improve their detonation and propulsion properties. A thorough review of the literature concerning the synthesis of such compounds[6–20] was conducted in our previous work.[21] Disappointingly, the limited synthetic capabilities in laboratories have restricted the qualitative and quantitative analysis of these potential HEDMs to droplet-combustion experiments, thermogravimetric analysis, fast pyrolysis studies, etc.[22–29]

In our previous study,[21] the thermal decomposition of newly synthesized bis(nitratomethyl)-1,3-bishomocubane was analyzed by using a fast pyrolyzer, coupled with rapid-scan FTIR spectroscopy at a heating rate of 100 °C s^{-1}. Analysis of the evolved gases showed that primary decomposition took place owing to O–NO_2 bond scission, which resulted in the formation of CO_2, N_2O, NO_2, CO, and water. Stud-

[a] S. Lal, Dr. S. Rajkumar, Prof. Dr. I. N. N. Namboothiri
Department of Chemistry
Indian Institute of Technology, Bombay
Mumbai 400076 (India)
Fax: (+91) 22-2576-7152, 2572-3480

[b] Dr. S. Rajkumar
Present address: School of Chemistry
University of Leeds, Leeds LS2 9JT (UK)

[c] A. Tare, Prof. Dr. A. Chowdhury
Department of Mechanical Engineering
Indian Institute of Technology Bombay
Mumbai 400076 (India)
Fax: (+91) 22-2572 6875
E-mail: arindra@iitb.ac.in

[d] Dr. S. Reshmi
Polymers and Special Chemicals Group, PCM Entity
Vikram Sarabhai Space Centre (VSSC)
Thiruvananthapuram, Kerala 695022 (India)

Supporting information for this article is available on the WWW under http://dx.doi.org/10.1002/asia.201402607.

ies on nitro-based cage compounds revealed that the most-favorable thermolysis pathway was the dissociation of a cage C–C bond, despite the presence of a C–NO_2 bond, which typically ruptures first during the decomposition of nitro-based compounds.[30]

Herein, we report a systematic investigation into the thermodynamic and thermal characteristics of three nitro-bishomocubane (BHC)-based compounds: nitromethyl-1,3-bishomocubane (NMBHC), nitromethylene-1,3-bishomocubane (NMyBHC), and bis-(nitromethyl)-1,3-bishomocubane (DNTMBHC). Ab initio methods were used to optimize their geometries and determine their thermodynamic characteristics, whilst thermogravimetry combined with FTIR spectroscopy was employed to elucidate their thermal behavior and to identify the thermal decomposition pathways. The detonation characteristics of these compounds, such as detonation pressure and detonation velocity, as well as propulsive performance parameters, such as specific impulse and density specific impulse, were calculated by using semi-empirical methods and equilibrium thermodynamics, respectively.

Results and Discussion

Synthesis of the Cage Compounds

Bishomocubanone **1**,[31,32] which was prepared in three steps from readily available dicyclopentadiene, was an excellent substrate for the synthesis of new nitro-based cage compounds **2–4** (Scheme 1). Treatment of ketone **1** with nitro-

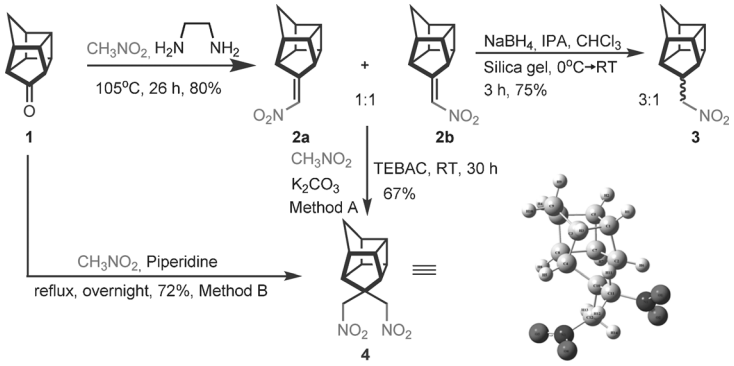

Scheme 1. Synthesis of NMBHC (**2**), NMyBHC (**3**), and DNTMBHC (**4**).

methane in the presence of ethylenediamine at 105 °C for 26 h provided NMBHC **2** as an inseparable mixture of isomers **2a** and **2b** (1:1 ratio, 80 % yield). Reduction of NMBHC **2** with sodium borohydride in a mixture of 2-propanol and $CHCl_3$ in the presence of silica gel furnished NMyBHC **3** as an inseparable mixture of isomers (3:1 ratio, 75 % yield). DNTMBHC **4** was synthesized by Michael addition of nitromethane to NMBHC **2** in the presence of K_2CO_3 and TEBAC (67 % yield, method A), as well as by a one-pot reaction of ketone **1** with nitromethane in the presence of piperidine (72 % yield, method B). The structures of compounds **2–4** were assigned by detailed analysis of their spectroscopic data. The structure of compound **4** was established by single-crystal X-ray analysis (Scheme 1 and the Supporting Information, Table S1).

Computational Methods

DFT analysis was performed with the B3LYP[33,34] exchange correlation functional in the Gaussian 09 suite of programs[35] and the 6-31G(d)[36] basis set to optimize the geometries and determine the thermochemical parameters of these compounds. This level of theory was selected owing to its capability of providing accurate values of thermochemical parameters for various compounds.[37–39] Diffuse functions were added to the basis set whilst calculating the bond-dissociation energies. The HoFs of the BHC-based compounds were calculated by using appropriate isodesmic reactions.[40] The isodesmic reactions for NMBHC, NMyBHC, and DNTMBHC are shown in Equations (1)–(3), respectively.

$$C_{11}H_{13}NO_2+CH_4 = C_8H_8+C_4H_9NO_2 \quad (1)$$

$$C_{11}H_{11}NO_2+2\,CH_4 = C_8H_8+C_2H_4+C_3H_7NO_2 \quad (2)$$

$$C_{12}H_{14}N_2O_4+2\,CH_4 = C_8H_8+2\,C_3H_7NO_2 \quad (3)$$

In these isodesmic reactions, the cage skeleton was fragmented and restructured to form cubane and the appropriate nitro-based compounds. The gas-phase HoFs of cubane, methane, *n*-nitropropane, *n*-nitrobutane, and ethylene were taken as 622.1,[4] −74.87,[41] −123.6,[41] −144.02,[41] and 52.7 kJ mol^{-1},[41] respectively. The densities of the cage hydrocarbons were calculated at the same level of theory by dividing the molar weights of the compounds by their respective molar volumes, which were determined on the basis of the 0.001 e bohr^{-3} density envelope by using the Monte-Carlo method.[42]

The ballistic properties of these compounds, such as vacuum-specific impulse (I_{sp}) and density vacuum specific impulse (ρI_{sp}), were calculated by using the NASA CEA (chemical equilibrium with applications) utility.[43] To assess the performance of these compounds as bipropellants with liquid oxygen as an oxidizer and as solid propellants with ammonium perchlorate as an oxidizer, the chamber pressure and exit-to-throat area ratio were taken as 1000 psi and 70:1, respectively. The heats of combustion of the compounds were calculated by assuming complete combustion in gaseous oxygen, as shown in Equations (4)–(6), respectively. The HoFs for water and CO_2 were taken to be −241.83 and −393.52 kJ mol^{-1}, respectively, from the NIST database.[41]

$$C_{11}H_{13}NO_2+13.25\,O_2 = 11\,CO_2+6.5\,H_2O+0.5\,N_2 \quad (4)$$

$$C_{11}H_{11}NO_2+12.75\,O_2 = 11\,CO_2+5.5\,H_2O+0.5\,N_2 \quad (5)$$

$$C_{12}H_{14}N_2O_4+13.5\,O_2 = 12\,CO_2+7\,H_2O+N_2 \quad (6)$$

The oxygen balance (OB),[44] defined as the percentage of intrinsic oxygen available for combustion, of a compound with molecular formula $C_aH_bO_cN_d$, is denoted by Equation (7).

$$OB = \frac{-32\left(a+{}^1\!/_4 b-{}^1\!/_2 c\right)}{MW}\times 100 \quad (7)$$

The detonation properties of these BHC-based compounds were calculated by using the Kamlet–Jacobs empirical correlation,[45] based on the maximum exothermicities of the detonation reactions. The maximum exothermicity principle states that, in any detonation reaction, the nitrogen content of the compound forms N_2 and the intrinsic oxygen present in the compound reacts first with hydrogen to form water, while the remaining reacts with carbon to form CO_2. The rest of the hydrogen and carbon form molecular hydrogen and solid carbon, respectively. The detonation pressure (P, in kbar) and detonation velocity (D in $km\,s^{-1}$) were calculated by using computationally estimated HoFs and densities with the empirical correlations shown in Equations (8) and (9), where ρ ($g\,cm^{-3}$) is the density, M_{av}($g\,mol^{-1}$) is the average molecular weight of the gaseous products, N ($mol\,g^{-1}$) is the number of moles of gaseous products per gram of explosive, and Q ($cal\,g^{-1}$) is the enthalpy of detonation.

$$P = 15.58\rho^2(NM_{av}^{1/2}Q^{1/2}) \quad (8)$$

$$D = 1.01\sqrt{(NM_{av}^{1/2}Q^{1/2})}(1+1.3\rho) \quad (9)$$

Thermodynamic, Ballistic, and Propulsive Properties

The optimized geometries of three cage hydrocarbons, NMBHC, NMyBHC, and DNTMBHC, are shown in Figure 1 and the coordinates are provided in the Supporting Information, Tables S2–S4. The bond lengths in these BHC-based compounds were subsequently examined (see the Supporting Information, Table S5). The lengths of the strained cage C–C bonds in the optimized geometry of NMBHC varied from 1.5297–1.5771 Å. The cage C–C bond lengths of DNTMBHC varied from 1.5269–1.5786 Å, which showed that the cage structure was not significantly affected by the addition of an additional nitromethyl group. The lengths of the C–NO_2 bonds in nitro-based compounds are of considerable interest owing to the possibility of thermal decomposition being initiated through C–N bond scission. The length of the C–NO_2 bond in NMBHC was calculated to be 1.5064 Å, similar to the C–NO_2 bonds in DNTMBHC (1.5058 and 1.5156 Å). The cage C–C bond lengths in NMyBHC varied from 1.4999–1.5959 Å. The C2–C10 and C4–C10 bonds in NMyBHC were shorter than the corresponding bonds in NMBHC and DNTMBHC, owing to sp^2 hybridization at the C10 atom and increased s character of the sp^2-hybridized orbital that was used to form the σ bond. The C–NO_2 bond in NMyBHC was 1.4521 Å, which was considerably shorter than those in NMBHC and DNTMBHC.

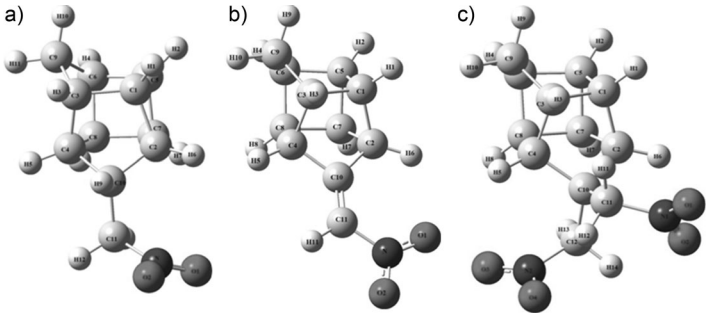

Figure 1. Optimized structures of NMBHC (a), NMyBHC (b), and DNTMBHC (c) at the B3LYP6-31G(d) level of theory.

A comparison of the bond angles (see the Supporting Information, Table S6) showed that all of the angles varied from the unstrained tetrahedral angle of 109.5°. The largest deviation from 109.5° was observed for angles that belonged to the cyclobutane structures within the cage, that is, ∢C5-C7-C8 (86.97°), ∢C5-C6-C8 (86.99°), and ∢C1-C5-C7 (87.1°) for NMBHC, ∢C1-C2-C7 (86.34°), ∢C1-C5-C7 (86.91°), and ∢C5-C7-C8 (86.99°) for NMyBHC, and ∢C5-C7-C8 (87.06°), ∢C5-C6-C8 (87.1°), and ∢C1-C2-C7-(87.14°) for DNTMBHC. We observed that the C–C bond lengths in the cage skeletons of these compounds varied from the ideal unstrained C–C bond length of 1.54 Å. Because the stabilities and bond-dissociation energies of the bonds were inversely proportional to the bond lengths in general, the most probable sites for bond cleavage were those at which the C–C bonds deviated the most from 1.54 Å.

The gas-phase HoFs of NMBHC, NMyBHC, and DNTMBHC were 199.55, 230.95, and 173.8 $kJ\,mol^{-1}$, respectively, whilst the specific gravities were 1.403, 1.468, and 1.352, respectively. Notably, the gas-phase HoF was utilized to calculate the ballistic and explosive properties. Since the liquid-phase and solid-phase HoFs were lower than the gas-phase HoF, the predicted ballistic and explosive performance would be higher than the actual performance. The higher HoF value of NMyBHC was conjectured to be owing to the presence of a double bond between the cage structure and the substituent. In all cases, the HoFs were lower than that of 1,3-bishomocubane, which was calculated to be 243.65 $kJ\,mol^{-1}$ at the same level of theory. We observed that the substitution of $-CH_2NO_2$ groups onto the BHC cage led to a decrease in HoF value.

Similar observations were also made by Zhang et al.[46] based on DFT calculations of the HoFs of cubane-based compounds with NO_2 substituents at the B3LYP/6-31G(d) level of theory. They reported that each subsequent addition of a NO_2 group led to a decrease in the HoF up to three substitutions, whilst the addition of further NO_2 groups led to an increase in HoF. The decrease in HoF from the parent molecule, cubane, was approximately 40 $kJ\,mol^{-1}$ for the

first NO_2 addition and another 20 kJ mol^{-1} for the second addition, similar to those for NMBHC and DNTMBHC. The HoF of NMyBHC was calculated to be 230.95 kJ mol^{-1}, which was almost similar to that of BHC and larger than those of NMBHC and DNTMBHC. A comparison of the IR frequencies that were obtained from vibrational analysis of the compounds at the B3LYP/6-31G(d) level of theory and the experimental vibrational frequencies is shown in Table 1. It is well-known that computationally calculated

Table 1. Major calculated vibrational frequencies of NMBHC, NMyBHC, and DNTMBHC.

E.F.[a] [cm^{-1}]	T.F.[b] [cm^{-1}]	S.F.[c] [cm^{-1}]	Vibrational mode
NMBHC			
1355	1393	1316	C–C ring stretch or C–H rocking
1383	1442	1363	NO_2 symmetrical stretch
1433	1498	1416	C–H scissoring
1553	1666	1574	NO_2 asymmetrical stretch
2857	3052	2884	C–H symmetrical stretch on ring CH_2 groups
2974	3129	2957	C–H ring stretch
NMyBHC			
1349	1403	1326	NO_2 symmetrical stretch
1520	1627	1538	NO_2 asymmetrical stretch
2855	3055	2887	C–H symmetrical stretch on ring CH_2
2984	3132	2960	C–H ring stretch
DNTMBHC			
1377	1432	1353	NO_2 symmetrical stretch
1424	1496	1414	C–H scissoring
1543	1664	1573	NO_2 asymmetrical stretch
2857	3056	2888	C–H symmetrical stretch on ring CH_2 groups
2986	3136	2964	C–H ring stretch

[a] E.F. = experimental frequency; [b] T.F. = theoretical frequency; [c] S.F. = scaled frequency.

frequencies are often larger than experimental frequencies, owing to the omission of a harmonic effect and the selection of basis set.[47] Therefore, it is desirable to use a scaling factor to improve the computed vibrational frequencies.

The scaling factors (λ_s) for the BHC-based compounds were calculated by using the least-squares method reported by Scott and Radom.[47] The method minimizes the residual error between several experimental and computational frequencies, chosen such that the intensities at those frequencies were significantly high. The λ_s value calculated by using this approach was 0.945, with a root-mean-square error of 21.94 cm^{-1}, which was close to the standard scaling factor (0.96) at this level of theory. The Supporting Information, Figures S1–S3, show a comparison of the experimental and calculated IR spectra of NMBHC, NMyBHC, and DNTMBHC, respectively. The symmetrical and asymmetrical NO_2 stretches gave rise to the prominent doublets at about 1400 cm^{-1}, whilst C–H stretches at about 3000 cm^{-1} were also evident in the spectra. The scaled thermodynamic properties, that is, internal energy, specific heat capacity at constant pressure, and entropy, were calculated at the DFT-B3LYP level of theory with the 6-31G(d) basis set (see the Supporting Information, Tables S7–S9) for NMBHC, NMyBHC, and DNTMBHC, respectively. As expected, all of the thermodynamic properties showed an increase in magnitude with increasing temperature. A comparison of various ballistic and explosive properties of the BHC-based energetic compounds is shown in Tables 2–4. Notably, DNTMBHC, a solid, was assumed to form a 30% solution (by mass) with RP1 in the calculation of its specific impulse.

As shown in Table 2, the specific impulse of NMBHC with liquid oxygen as an oxidizer was marginally higher than that of NMyBHC and marginally lower than that of DNTMBHC; all of the values were slightly lower than that of the widely used liquid fuel RP1 under similar conditions. However, the density specific impulses of NMBHC and NMyBHC were approximately 75 s higher than that of RP1, whilst that of a DNTMBHC/RP1 mixture was 20 s higher, thus indicating the possible performance of these compounds under volume-limited conditions. The improvement in density specific impulses was significant compared to the previously studied compound, bis(nitrato-methyl)-bishomocubane.[21]

Table 2. Comparison of predicted propulsive properties as liquid bipropellants.[a]

Propellant	Mixture ratio	I_{sp} (s)	ρI_{sp} (s)	CCT[b] [K]
RP1	2.58:1	366.2	374.3	3666.4
NMBHC	1.51:1	362.3	446.4	3801.2
NMyBHC	1.46:1	359.4	450.6	3827.1
DNTMBHC+RP1	2.15:1	364.2	393.4	3682.6

[a] Oxidizer: liquid oxygen, chamber pressure: 1000 psi, area ratio: 70:1; [b] CCT = combustion chamber temperature. I_{sp}: specific impulse

The possibility of replacing HTPB as a non-energetic component in ammonium-perchlorate-based solid propellant formulations was also investigated (Table 3). The compounds showed improvements of 25–30 s in specific impulse over HTPB, thus indicating their promise as replacement monomers for HTPB as a binder.

As shown in Table 4, the oxygen balance in all three compounds was negative, thus confirming that these were

Table 3. Predicted propulsive properties of the synthesized compounds as solid propellants (20%) with ammonium perchlorate (80%).[a]

Propellant	I_{sp} (s)
HTPB	274.6
NMBHC	299.0
NMyBHC	299.1
DNTMBHC	307.2

[a] Chamber pressure: 1000 psi, area ratio: 70:1. I_{sp}: specific impulse

Table 4. Predicted explosive properties of the synthesized compounds.[a]

Propellant	OB [%]	D.P. [GPa][b]	D.V. [km s^{-1}][c]
NMBHC (g)	−221.99	10.14	5.19
NMyBHC (g)	−215.87	10.47	5.19
DNTMBHC (g)	−172.8	11.78	5.66
RDX (g)	−21.622	35.14	8.93

[a] Calculated by using the Kamlet–Jacobs correlation; [b] D.P. = detonation pressure; [c] D.V. = detonation velocity.

oxygen-deficient compounds and should be mixed with oxidizers to assist combustion and are not suitable candidates as monopropellants. The heats of combustion of NMBHC, NMyBHC, and DNTMBHC, as calculated by assuming complete combustion, were 31.94, 31.16, and 26.38 MJ kg^{-1}, respectively. The highest detonation pressure and detonation velocity among these compounds were determined for DNTMBHC, owing to the presence of an additional NO_2 group in its cage structure. The variation in detonation pressure and detonation velocity among the BHC-based compounds showed that these parameters were dependent on the presence of NO_2 groups and decreased as the number of NO_2 groups in the BHC cage skeleton decreased. A quick comparison of the detonation properties with a standard explosive (RDX) revealed that these compounds were not explosive in nature, owing to their oxygen-deficient and carbon-rich structures. Based on previous studies of families of substituted cage hydrocarbons, the addition of further nitro groups onto the bishomocubane cage would certainly improve the oxygen balance and detonation properties of the molecule and will be the subject of future synthesis efforts within our group.

The adiabatic flame temperatures (T_{ad}) of the BHC-based compounds were calculated at a pressure of 69 bar with liquid oxygen as the oxidizer and at different equivalence ratios. Assuming complete oxidation of the reactant species, we found that the T_{ad} values varied from 3400–3850 K, with the maximum values occurring at slightly rich mixtures, that is, for equivalence ratios higher than the stoichiometric value. The highest calculated T_{ad} values for NMBHC, NMyBHC, and DNTMBHC were 3827 K ($\varphi = 1.25$), 3850.4 K ($\varphi = 1.27$), and 3802.4 K ($\varphi = 1.29$), respectively, which were approximately 200 K higher than that for RP1. The high adiabatic flame temperatures were attributed to the high HoFs of these compounds.

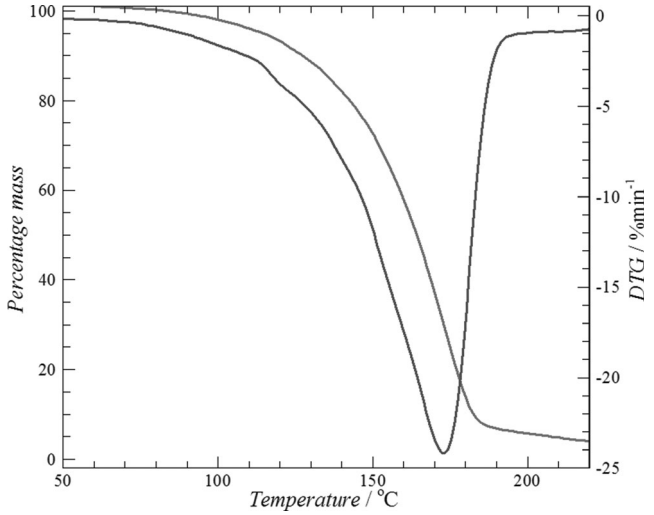

Figure 2. TG/DTG of NMBHC at 10 K min^{-1}.

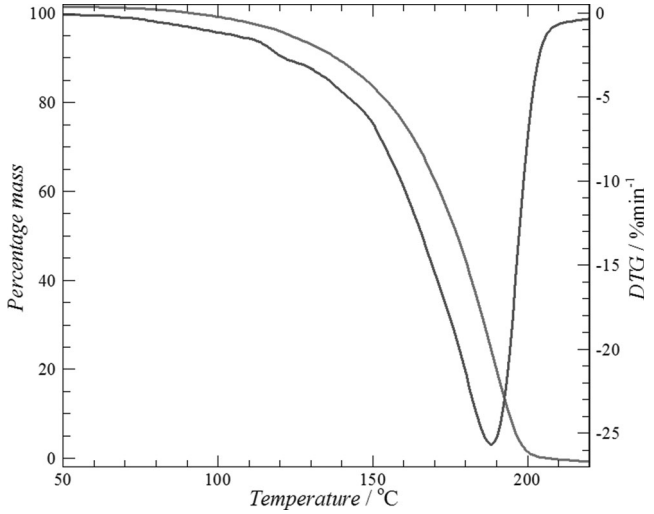

Figure 3. TG/DTG of NMyBHC at 10 K min^{-1}.

Thermal Analysis

NMBHC, NMyBHC, and DNTMBHC were subjected to slow pyrolysis under an inert atmosphere and their thermal characteristics, that is, their TGA and DTG curves, are shown in Figures 2–4, respectively.

Under standard conditions, both NMBHC and NMyBHC were viscous liquids, whereas DNTMBHC existed as a white crystalline solid. As shown in Figure 2, the mass-loss curve of NMBHC had an extrapolated onset temperature of 148 °C and an extrapolated end temperature of 183 °C. Approximately 95 % mass loss occurred in a single stage; the DTG signal showed a peak at 173 °C. The onset temperature was lower than that of the parent compound, 1,3-bishomocubane (168 °C), and its poly-nitro-derivatives, which decomposed at temperatures that were approximately 100 °C higher.[48] The previously studied bis(nitrato-methyl)-bishomocubane had a low decomposition onset temperature of 140 °C.

Several iodo derivatives of cubane also had onset temperatures within the range 103–168 °C,[49] with the exception of an iodo-acid derivative, which had the highest onset temperature of 206 °C. On further investigation by using DSC, some of the iodo-based compounds revealed that the mass loss was owing to evaporation or sublimation instead of thermal decomposition. Thorough analysis of the FTIR spectra of the evolved gas-phase species during the thermolysis of NMBHC at 143 °C and 178 °C (see the Supporting Information, Figure S4) confirmed the sole presence of NMBHC, with symmetrical and asymmetrical NO_2 stretches, as well as C–H bands, which accurately matched with the condensed-phase FTIR spectra of NMBHC. The lack of species with smaller molecular weights, such as NO_2, NO, CO, and CO_2, which are possible by-products of C–NO_2 bond scission, as well as various smaller hydrocarbons, such as ethylene, acetylene, or cyclic hydrocarbons, which could be produced by ring opening, ruled out the condensed-phase decomposition of NMBHC.

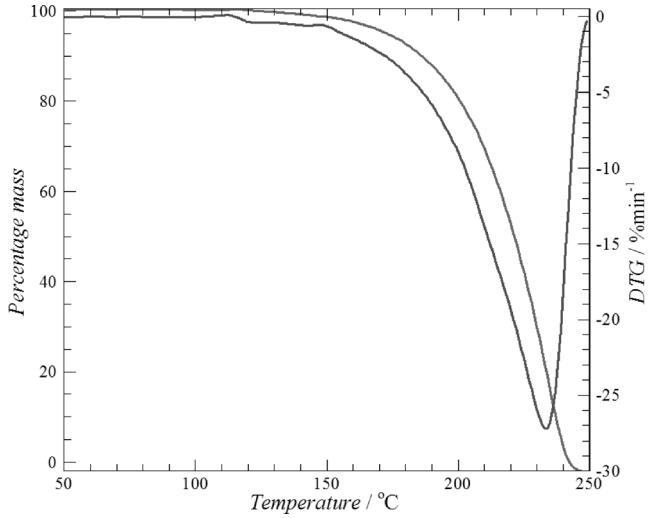

Figure 4. TG/DTG of DNTMBHC at 10 K min^{-1}.

The TGA signal for the thermolysis of NMyBHC (Figure 3) was similar in nature to that of NMBHC. The extrapolated onset temperature was calculated to be 160 °C, which was approximately 12 °C higher than that of NMBHC, thus showing that NMyBHC was thermally more stable than NMBHC and the previously studied bis(nitratomethyl)-bishomocubane.[21] Mass loss occurred in a single stage and the DTG signal showed a prominent peak at 188 °C and an extrapolated end temperature, that is, the extrapolated temperature from the TGA signal at which the mass loss is over, of 198 °C. The gas-phase FTIR spectra (see the Supporting Information, Figure S5) at 155 °C and 194 °C showed the presence of NMyBHC in the gas phase. The symmetrical and asymmetrical NO_2 stretches, as well as the C–H stretches, matched with those of NMyBHC. However, the C–H scissoring band at approximately 1450 cm^{-1} in the condensed-phase spectrum was absent in the gas phase.

The mass-loss and DTG curves of DNTMBHC (Figure 4) showed that it underwent a single-stage mass loss with an extrapolated onset temperature of 205 °C, thus establishing it as the most thermally stable compound of the three nitro-BHC-based compounds. The extrapolated end temperature of DNTMBHC was 242 °C. The difference between the onset and end temperatures of NMBHC, NMyBHC, and DNTMBHC were 35 °C, 38 °C, and 37 °C, respectively. A similar temperature difference has been observed for iodocubane-based compounds.[49] The DTG signal for DNTMBHC showed a peak at 234 °C. The Supporting Information, Figure S6, shows FTIR spectra of the products that were formed during the thermolysis of DNTMBHC at 199 °C and 238 °C, which confirmed that DNTMBHC was the sole compound present in the gas phase. Since the melting point of DNTMBHC was experimentally determined to be between 95–97 °C, the process revealed by the TGA signal was postulated to be the evaporation of DNTMBHC.

The Kissinger–Akihara–Sunose isoconversional method,[50] in conjunction with the Coats–Redfern method,[51] and aided by 12 various kinetic models, including reaction-order-based models, diffusion-based models, contracting surface-based models, and power-law-based models, was used to extract the kinetic parameters for the three compounds from the TGA data (also see the Experimental Section).

Thus, we have established that all three compounds underwent evaporation under thermal stress at the given heating rates. This fact was also evident from kinetic analysis by using the isoconversional method (Figure 5). The variation

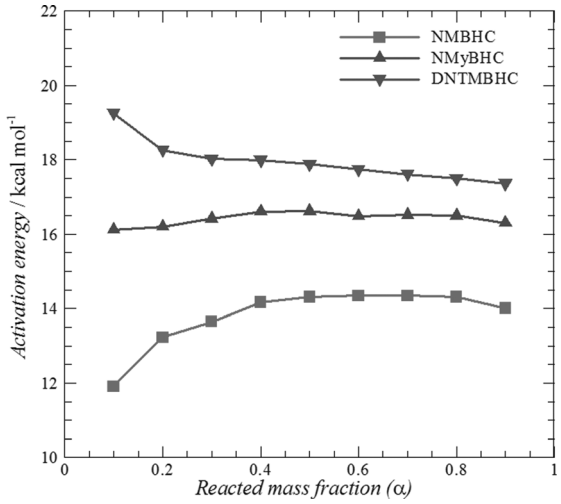

Figure 5. Variation in activation energy with reacted mass fraction (α).

in activation energy was minimal for all three compounds, thereby reiterating that a single physical process governed their thermal behavior. The activation energies of evaporation were determined by averaging the values from $\alpha = 0.3$–0.8 (Table 5).

Table 5. Experimental Arrhenius parameters for non-isothermal thermolysis of NMBHC, NMyBHC, and DNTMBHC.[a]

Propellant	Activation energy (E_a) [kJ mol^{-1}]	Frequency factor (A) [min^{-1}]
NMBHC	58.84	1.52E+06
NMyBHC	69.19	1.31E+07
DNTMBHC	74.47	7.90E+06

[a] Calculated by using the Kissinger–Akihara–Sunose method from the TGA data.

Next, the activation energies were used to determine the "proper" values of the pre-exponential factors by using the kinetic compensation effect. The activation energies showed an increasing trend from NMBHC to NMyBHC and DNTMBHC. The activation energies of evaporation of NMBHC, NMyBHC, and DNTMBHC (58.8, 69.2, and 74.5 kJ mol^{-1}, respectively) were similar to those of trinitroa-

zetidine (81 kJ mol^{-1})[52] and nitroglycerine (57.8–80.3 kJ mol^{-1}),[53] which are similar energetic materials. The pre-exponential factors of these compounds, although similar to that of nitroglycerin, were several orders of magnitudes smaller than that of trinitroazetidine. These data will be useful in future numerical simulations entailing the combustion of liquid bipropellant combinations whilst determining the mass evaporation rates of droplets.

The initiation of decomposition of the three nitro-BHC-based materials was studied by using computational techniques to further analyze their thermal stability. During these calculations, diffuse functions were used for the optimization to lend further credibility to the bond-dissociation energy (BDE) values. C–NO_2 bond scission typically acts as the initiation reaction for nitro-alkanes and nitro-arene compounds, such as nitromethane, nitroethane,[54] trinitrotoluene, and nitrobenzene.[55] However, decomposition of the highly strained cage compounds may also proceed through breaking of the ring C–C bonds. Thus, the possibility of decomposition of NMBHC and DNTMBHC was studied through cleavage of the C–NO_2 bond, cleavage of the longest cage C–C bond, and cleavage of the second-longest cage C–C bond (Scheme 2–4).

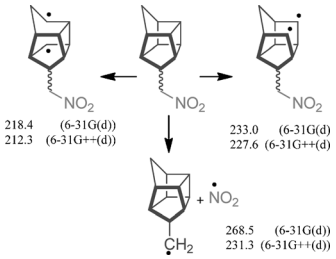

Scheme 2. Thermal decomposition pathways and calculated BDEs (in kJ mol^{-1}) of NMBHC.

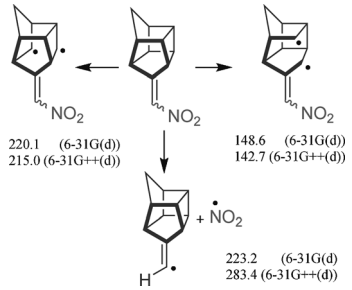

Scheme 3. Thermal decomposition pathways and calculated BDEs (in kJ mol^{-1}) of NMyBHC.

Although the C–NO_2 BDEs for NMBHC and DNTMBHC were higher than the ring C–C BDEs without the diffuse functions, the values were comparable to the C–C BDEs when diffuse functions were used. Thus, conclusive evidence for the dominance of the ring-fragmentation pathways over traditional NO_2 extraction, as observed during the simulated thermal decomposition of nitro-cubanes,[30]

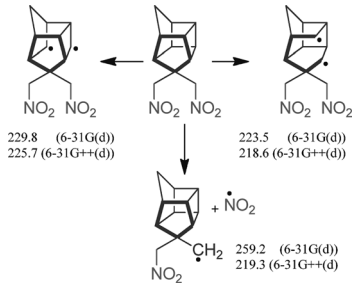

Scheme 4. Thermal decomposition pathways and calculated BDEs (in kJ mol^{-1}) of DNTMBHC.

could not be obtained for these compounds. In addition, the C–C bond-dissociation energies for both of the strained bonds that involved the cyclobutane rings were relatively similar for both compounds, further negating the choice of a dominant pathway during the ring scission. Moreover, the bond-dissociation energies were similar to the activation energy of decomposition of the dinitro-carboxylic acid of BHC.[54] Another interesting facet was the significantly lower bond-dissociation energy of the C–C bond in the cyclobutane ring adjacent to the C=C bond, which may be caused by allylic stabilization of the resultant diradical. Notably, these conclusions based on numerical evaluation of the bond-dissociation energies need to be verified by calculation of the activation energies with suitably optimized transition states and through experimental evidence involving gas-phase pyrolysis, which is the subject of future endeavors within our group.

Conclusions

Three new polycyclic nitro-substituted cage compounds—NMBHC, NMyBHC, and DNTMBHC—were synthesized and analyzed by using ab initio methods, semi-empirical methods, thermogravimetric analysis, and IR spectroscopy. NMBHC and NMyBHC were liquids under standard conditions and have potential application as direct replacements for RP1, owing to their improved density specific impulses (by approximately 75 s). DNTMBHC may be utilized as an additive in RP1, thereby providing an improvement in density specific impulse of 20 s. These compounds are also potential monomer units for energetic binders in solid propellant formulations, thereby showing an improvement of 25 s over HTPB. NMBHC, NMyBHC, and DNTMBHC also possessed relatively high heats of formation of 199.55, 230.95, and 173.8 kJ mol^{-1} and specific gravities of 1.403, 1.468, and 1.352, respectively. These compounds also possessed high heats of combustion of approximately 30 MJ kg^{-1}. NMBHC, NMyBHC, and DNTMBHC evaporated under thermal stress, as verified by FTIR spectroscopy, with activation energies of 58.8, 69.2, and 74.5 kJ mol^{-1}, respectively, and pre-exponential factors of 1.5×10^{6}, 1.3×10^{7}, and 7.9×10^{6} min^{-1}, respectively. Computational studies did not conclusively establish the precedence of scission of the

strained ring C–C bonds over C–NO_2 bond scission for NMBHC and DNTMBHC, as observed in similar nitro-substituted cage compounds.

Experimental Section

Thermogravimetric analysis (TGA) of the compounds was performed on a Netzsch TG209 F1 Libra thermogravimetric analyzer, which was coupled to a Bruker Vertex 80 FTIR spectrometer—along with its accompanying optics—through a transfer line to identify the evolved gases. Briefly, the compound (approximately 1 mg) was heated in an open Al_2O_3 crucible under a constant nitrogen (99.995% purity) flow at a purge flow rate of 120 mL min^{-1} The protective purge flow rate was set to 10 mL min^{-1}, which was adequate for effectively transferring the gases from the TGA module into the FTIR spectrometer through a heated PTFE transfer tube, which was maintained at 210 °C. The gases were transported into a heated gas cell, which was equipped with two KBr windows and two ZnSe windows, at 190 °C. The FTIR spectra of the gases were recorded from 3750–650 cm^{-1}, with a spectroscopic resolution of 4 cm^{-1}. The compounds were heated from 30–250 °C at three heating rates of 2.5, 5, and 10 K min^{-1}. These heating rates were chosen to determine the activation energies and pre-exponential factors associated with the thermochemical processes that occurred during the TGA runs. The variation in activation energy with reacted mass fraction (α) was determined by using the Kissinger–Akahira–Sunose method,[50] which is a robust integral isoconversional method. The activation energies were used to determine the pre-exponential factors utilizing the kinetic compensation effect, where the multiple activation energy and pre-exponential factor doublets were determined by using standard reaction models (see the Supporting Information, Table S10).[50] The Coats–Redfern approximation method was used to analyze the non-isothermal mass-loss data.[51]

The melting points were recorded on a Buchi(M-560) melting point apparatus and are uncorrected. IR spectra were recorded on Impact 400/Nicolet or PerkinElmer Spectrum One FT spectrometer. NMR spectra (^1H and ^{13}C) were recorded on Bruker 400 and 500 MHz spectrometers by using TMS as an internal standard. Coupling constants (J) are reported in Hz. Mass spectra were recorded at 60–70 eV on a Micromass Q-TOF mass spectrometer in ESI mode. X-ray data were collected on a Nonius MACH 3 diffractometer that was equipped with graphite-monochromated $Mo_{K\alpha}$ radiation. The structures were solved by using direct methods (SHELXS97) and refined by full-matrix least-squares against F^2 by using SHELXL97 software.

*6-(Nitromethylene)pentacyclo[5.3.0.0^{2,5}.0^{3,9}.0^{4,8}]decane(**2**)*

Ketone **1** (500 mg, 3.42 mmol) and ethylenediamine (0.023 mL, 20.5 mg, 0.342 mmol) were added to nitromethane (15.4 mL, 17.62 g, 0.287 mol) under a nitrogen atmosphere. The reaction mixture was heated at reflux for 26 h, before being allowed to cool to room temperature and acidified with 10% HCl. The layers were separated and the aqueous layer was extracted with CH_2Cl_2 (5×10 mL). The combined organic layer was washed with water (4×30 mL) and brine (20 mL), dried over anhydrous sodium sulfate, and concentrated in vacuo. The crude residue was purified by silica gel column chromatography (petroleum ether) to afford pure nitroalkene **2** as a yellow liquid (517 mg, 80% yield, ≈1:1 mixture of inseparable isomers).

^1H NMR ($CDCl_3$, 400 MHz): δ = 6.85, 6.84 (s, 2H; both isomers), 4.16 (t, J = 4.0 Hz, 1H; one isomer), 3.98–3.97 (m, 1H; the second isomer), 3.06–2.79 (m, 14H; both isomers), 1.79,1.53 ppm (ABq, J = 11.0 Hz, 4H; both isomers); ^{13}C NMR ($CDCl_3$, 100 MHz): δ = 166.21 (s), 165.90 (s), 126.42 (d), 125.46 (d), 50.79 (d), 48.20 (d), 48.03 (d), 47.75 (d), 44.18 (d), 43.48 (d), 42.99 (d), 42.75 (d), 42.50 (d), 41.31 (d), 41.11 (d), 41.09 (d), 41.00 (d), 40.94 (2×t), 39.94 (d), 37.94 (d), 37.21 ppm (d); IR (film): $\tilde{\nu}$ = 3054 (m), 2984 (m), 2855 (w), 1520 (m), 1422 (m), 1349 (m), 1265 cm^{-1} (s); MS (ES+): m/z (%): 212 (70) $[M+Na]^+$, 190 (9) $[M+H]^+$, 173 (100), 172 (68), 156 (58), 143 (27); HRMS (ES+): m/z calcd for $C_{11}H_{11}NO_2Na$: 212.0687; found: 212.0691.

*6-(Nitromethane)pentacyclo[5.3.0.0^{2,5}.0^{3,9}.0^{4,8}]decane (**3**)*

Silica gel (1.52 g, 200–400 mesh) was added to a solution of nitroalkenes **2a** and **2b** (145 mg, 0.77 mmol) in 2-propanol (2.3 mL) and $CHCl_3$ (12.2 mL). $NaBH_4$ (119 mg, 3.15 mmol) was added over 5 min under stirring and the mixture was cooled to 0 °C. Then, the reaction mixture was stirred at room temperature for 2 h, washed with dilute HCl (2×10 mL), filtered, and the filtrate was extracted with CH_2Cl_2 (5×10 mL). The combined organic layer was washed with water (20 mL) and brine (10 mL), dried over anhydrous sodium sulfate, and concentrated in vacuo. The crude residue was purified by column chromatography on silica gel (petroleum ether) to afford pure nitroalkane **3** as a yellow liquid (110 mg, 75% yield, ≈3:1 mixture of inseparable isomers).

^1H NMR ($CDCl_3$, 400 MHz): δ = 4.42, 4.37 (ABqd, J = 12.0, 7.6 Hz, 2H; major isomer), 4.04, 4.01 (ABqd, J = 12.0, 7.8 Hz, 2/3H; minor isomer), 2.85–2.40 (m, 9H; major+minor isomers), 1.37–1.66 ppm (m, 2H; major+minor isomers); ^{13}C NMR ($CDCl_3$, 100 MHz; major isomer): δ = 76.44 (t), 49.98 (d), 49.82 (d), 44.65 (d), 43.44 (d), 43.09 (d), 41.58 (d), 40.58 (d), 39.99 (d), 39.65 (d), 38.31 ppm (t); ^{13}C NMR ($CDCl_3$, 100 MHz; minor isomer): δ = 75.23 (t), 50.10 (d), 49.16 (d), 47.55 (d), 43.15 (d), 42.69 (d), 40.89 (d), 40.15 (d), 38.17 ppm (t); IR (film): $\tilde{\nu}$ = 2974 (s), 2857 (w), 1553 (vs), 1433 (w), 1383 (m), 1355 (w), 1265 (w), 1196 (w), 738 cm^{-1} (s); MS (ES+): m/z (%): 214 (54) $[M+Na]^+$, 158 (100), 141 (10), 106 (69); HRMS (ES+): m/z calcd for $C_{11}H_{13}NO_2Na$: 214.0844; found: 214.0854.

*6,6-Bis(Dinitromethane)pentacyclo[5.3.0.0^{2,5}.0^{3,9}.0^{4,8}]decane (**4**)*

Method A: A solution of nitroalkene **2** (191 mg, 1 mmol) in nitromethane (15 mL, excess) was added to a solution of K_2CO_3 (187 mg, 1.35 mmol) and triethyl benzyl ammonium chloride (TEBAC, 31 mg, 0.13 mmol) in nitromethane (10 mL, excess) and the mixture was stirred vigorously at room temperature for 30 h. The mixture was treated with brine (50 mL) and the yellow solution was extracted with CH_2Cl_2 (5× 15 mL). The combined organic layer was washed with water (15 mL) and brine (15 mL), dried over anhydrous sodium sulfate, and concentrated in vacuo. The crude residue was purified by column chromatography on silica gel (EtOAc/petroleum ether, 0–2%) to afford almost-pure compound **4** as a viscous yellow liquid, which was further purified by crystallization from petroleum ether (colorless solid, 168 mg, 67% yield).

Method B: Cage ketone **1** (400 mg, 2.74 mmol) and piperidine (138 mg, 1.64 mmol) were added to nitromethane (25 mL, excess) at room temperature and the reaction mixture was heated at reflux overnight. The mixture was cooled to ambient temperature and washed with 10% HCl. The layers were separated and the aqueous layer was extracted with CH_2Cl_2 (5×30 mL). The combined organic layer was washed with water (4× 30 mL) and brine (20 mL), dried over anhydrous sodium sulfate, and concentrated in vacuo. The crude residue was purified by column chromatography on silica gel (petroleum ether) to afford pure dinitroalkane **4** as a colorless solid (494 mg, 72% yield).

M.p. 95–97 °C; ^1H NMR ($CDCl_3$, 400 MHz): δ = 4.83, 4.65 (ABq, J = 13.5 Hz, 2H), 4.62 (d, J = 12.8 Hz, 1H), 4.23 (d, J = 12.8 Hz, 1H), 3.05–2.97 (m, 1H), 2.95–2.72 (m, 4H), 2.78–2.70 (m, 2H), 2.45–2.40 (m, 1H), 1.40 (d, J = 11.4 Hz, 1H), 1.20 ppm (d, J = 11.4 Hz, 1H); ^{13}C NMR ($CDCl_3$, 100 MHz): δ = 75.28 (t), 74.51 (t), 56.57 (s), 53.13 (d), 45.74 (d), 42.27 (d), 41.91 (d), 39.54 (d), 38.32 (d), 38.26 (d), 37.89 ppm (t); IR (KBr): $\tilde{\nu}$ = 2986 (s), 2228 (m), 2857 (w), 1543 (vs), 1424 (m), 1377 (m), 910 (vs), 733 cm^{-1} (vs); MS (ES+): m/z (%): 251 (100) $[M+H]^+$; HRMS: m/z calcd for $C_{12}H_{15}N_2O_4$ $[M+H^+]$: 251.1032; found: 251.1021.

CCDC 1006407 (**4**) contains the supplementary crystallographic data for this paper. These data can be obtained free of charge from The Cambridge Crystallographic Data Centre via www.ccdc.cam.ac.uk/data_request/cif.

Acknowledgements

We acknowledge financial support from the Indian Space Research Organization (ISRO) and the Armament Research and Development Board (ARDB), as well as from the Industrial Research and Consultancy Center (IRCC) at the Indian Institute of Technology, Bombay. We acknowledge the discussions with Prof. K. N. Ninan regarding the synthesis of the compounds.

[1] J. P. Agrawal, *Prog. Energy Combust.* **1998**, *24*, 1–30.
[2] P. E. Eaton, T. W. Cole, *J. Am. Chem. Soc.* **1964**, *86*, 3157–3158.
[3] P. E. Eaton, M. X. Zhang, *Proceedings of 9th ONR Propulsion Meeting*, State University of New York, Buffalo, NY **1996**, 111.
[4] B. D. Kybett, S. Carroll, P. Natalis, D. W. Bonnell, J. L. Margrave, J. L. Franklin, *J. Am. Chem. Soc.* **1966**, *88*, 626.
[5] P. E. Eaton, F. Alberici, L. Cassar, F. Monti, C. Neri, N. Nodari, Patent number US4943302A, **1990**, USA.
[6] A. P. Marchand, *Advances in theoretically interesting molecules*, JAI Press, Greenwich, **1989**.
[7] P. E. Eaton, Y. Xiong, R. Gilardi, *J. Am. Chem. Soc.* **1993**, *115*, 10195–10202.
[8] P. E. Eaton, *Proceedings of 7th ONR Propulsion Meeting*, State University of New York, Buffalo, NY **1994**, 117–129.
[9] A. P. Marchand, Z. Liu, D. Rajagopal, V. D. Sorokin, F. Zaragoza, A. Zope, *Proceedings of the 7th ONR Propulsion Meeting*, State University of New York, Buffalo, NY **1994**, 82–90.
[10] R. Butcher, A. Bashir-Hashemi, R. Gilardi, *J. Chem. Crystallogr.* **1997**, *27*, 99–107.
[11] A. K. Sikder, N. Sikder, *J. Hazard. Mater.* **2004**, *112*, 1–15.
[12] L. E. Fried, M. R. Manaa, P. F. Pagoria, R. L. Simpson, *Annu. Rev. Mater. Res.* **2001**, *31*, 291–321.
[13] P. F. Pagoria, G. S. Lee, A. R. Mitchell, R. D. Schmidt, *Thermochim. Acta* **2002**, *384*, 187–204.
[14] P. E. Eaton, R. L. Gilardi, M. X. Zhang, *Adv. Mater.* **2000**, *12*, 1143–1148.
[15] A. P. Marchand, *Chem. Rev.* **1989**, *89*, 1011–1033.
[16] A. P. Marchand, *Aldrichimica Acta* **1995**, *28*, 95–104.
[17] G. Mehta, H. S. P. Rao, *Tetrahedron* **1998**, *54*, 13325–13370.
[18] P. E. Eaton, *Angew. Chem. Int. Ed. Engl.* **1992**, *31*, 1421–1436; *Angew. Chem.* **1992**, *104*, 1447–1462.
[19] K. A. Lukin, J. Li, P. E. Eaton, N. Kanomata, J. R. Hain, E. Punzalan, R. Gilardi, *J. Am. Chem. Soc.* **1997**, *119*, 9591–9602.
[20] A. P. Marchand, *Kem. Ind.* **2002**, *51*, 51.
[21] S. Rajkumar, R. S. Choudhari, A. Chowdhury, I. N. N. Namboothiri, *Thermochim. Acta* **2013**, *563*, 38–45.
[22] G. D. Roy, *J. Propul. Power* **2000**, *16*, 546–551.
[23] T. X. Li, D. L. Zhu, C. K. Law, *J. Propul. Power* **1998**, *14*, 45–50.
[24] C. K. Law, *49th AIAA Aerospace Sciences Meeting including the New Horizons Forum and Aerospace Exposition*, American Institute of Aeronautics and Astronautics, Orlando, Florida, 4–7 January **2011**.
[25] H. D. Martin, T. Urbanek, P. Pfohler, R. Walsh, *J. Chem. Soc. Chem. Commun.* **1985**, 964–965.
[26] H. D. Martin, T. Urbanek, R. Walsh, *J. Am. Chem. Soc.* **1985**, *107*, 5532–5534.
[27] C. Segal, S. Pethe, K. R. Williams, *Combust. Sci. Technol.* **2001**, *163*, 229–244.
[28] Z. Li, S. L. Anderson, *J. Phys. Chem. A* **2003**, *107*, 1162–1174.
[29] F. J. Owens, *THEOCHEM* **1999**, *460*, 137–140.
[30] J. Zhang, H. Xiao, *J. Chem. Phys.* **2002**, *116*, 10674–10683.
[31] I. N. N. Namboothiri, N. K. Meher, S. Chavan, B. Sahu, O. P. Oommen, T. L. Varghese, S. Reshmi, K. N. Ninan, *5th International High Energy Materials Conference*, Hyderabad, India, 23–25 November **2005**.
[32] a) R. B. Woodward, T. J. Katz, *Tetrahedron Lett.* **1959**, *1*, 19–21; b) R. C. Cookson, J. Hudec, R. O. Williams, *Tetrahedron Lett.* **1960**, *1*, 29–32.
[33] A. D. Becke, *J. Chem. Phys.* **1992**, *97*, 9173–9177.
[34] C. Lee, W. Yang, R. G. Parr, *Phys. Rev. B* **1988**, *37*, 785–789.
[35] Gaussian 09, Revision A.1, M. J. Frisch et al., Gaussian, Inc., Wallingford CT, **2009**.
[36] P. C. Hariharan, J. A. Pople, *Theor. Chim. Acta* **1973**, *28*, 213.
[37] B. M. Rice, S. V. Pai, J. Hare, *Combust. Flame* **1999**, *118*, 445–458.
[38] Z. X. Chen, J. M. Xiao, H. M. Xiao, Y. N. Chiu, *J. Phys. Chem. A* **1999**, *103*, 8062–8066.
[39] L. A. Curtiss, K. Raghavachari, P. C. Redfern, J. A. Pople, *J. Chem. Phys.* **1997**, *106*, 1063–1079.
[40] E. Lewars, *Introduction to the Theory and Applications of Molecular and Quantum Mechanics*, Kluwer Academic Publication, Dordrecht, **2003**.
[41] NIST Chemistry Webbook, available at http://webbook.nist.gov/chemistry/.
[42] K. E. Gutowski, J. D. Holbrey, R. D. Rogers, D. A. Dixon, *J. Phys. Chem. B* **2005**, *109*, 23196–23208.
[43] S. Gordon, B. J. McBride, NASA Reference Publication, **1996**, 1311.
[44] J. Akhavan, *The Chemistry of Explosives*, *2nd ed.*, Royal Society of Chemistry, Cambridge, **2004**.
[45] M. J. Kamlet, S. J. Jacobs, *J. Chem. Phys.* **1968**, *48*, 23–35.
[46] J. Zhang, H. Xiao, X. Gong, *J. Phys. Org. Chem.* **2001**, *14*, 583–588.
[47] A. P. Scott, L. Radom, *J. Phys. Chem.* **1996**, *100*, 16502–16513.
[48] D. I. Weinstein, J. Alster, A. P. Marchand, *Thermochim. Acta* **1986**, *99*, 133–137.
[49] J. R. Griffiths, J. Tsanaktsidis, G. P. Savage, R. Priefer, *Thermochim. Acta* **2010**, *499*, 15–20.
[50] S. Vyazovkin, A. K. Burnham, J. M. Criado, L. A. Pérez-Maqueda, C. Popescu, N. Sbirrazzuoli, *Thermochim. Acta* **2011**, *520*, 1–19.
[51] A. W. Coats, J. P. Redfern, *Nature* **1964**, *201*, 68–69.
[52] M. Sućeska, S. M. Mušanić, I. F. Houra, *Thermochim. Acta* **2010**, *510*, 9–16.
[53] A. S. Tompa, *J. Hazard. Mater.* **1980**, *4*, 95–112.
[54] P. Gray, A. D. Yoffe, L. Roselaar, *Trans. Faraday Soc.* **1955**, *51*, 1489–1497.
[55] J. Shao, X. Cheng, X. Yang, *Struct. Chem.* **2006**, *17*, 547–550.

Received: June 4, 2014
Revised: July 11, 2014
Published online: ■■ ■■, 0000

Energetic Materials

Sohan Lal, Sundaram Rajkumar, Amit Tare, Sasidharakurup Reshmi, Arindrajit Chowdhury, Irishi N. N. Namboothiri* ___ ▮▮▮▮–▮▮▮▮

Nitro-Substituted Bishomocubanes: Synthesis, Characterization, and Application as Energetic Materials

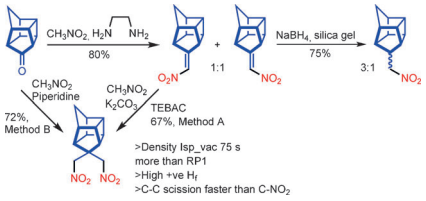

Cube runner: Nitro-bishomocubanes, readily synthesized from bishomocubanone, exhibited high positive heats of formation, heats of combustion, and specific impulses and hold potential as alternatives to conventional fuel RP1.